ORIGINAL PAPER

Preparation of three-dimensional cellulose objects previously swollen in a DMAc/LiCl solvent system

Jasmina Obradovic · Holger Wondraczek · Pedro Fardim · Lippo Lassila · Patrick Navard

Abstract Three-dimensionally shaped cellulosic objects were produced via a two-step procedure: swelling of softwood pulp (93 % cellulose; 4.5 % hemicellulose; 54 % crystallinity) in DMAc/LiCl followed by moulding. Swollen cellulose pulp in the form of gel was solidified with two different anti-solvents: distilled water and a combination of 2-propanol and deionized water. The solid cellulose material was further moulded in a custom-built prototype mould. The role of the anti-solvent was to solidify the swollen cellulose fibres and prepare mouldable solid specimens. The anti-solvent was chosen based on the following criteria, viz., recoverability, stable chemical reactivity, availability, cost and previous research in the anti-solvent area. The choice of solidification solvent had a great influence on the structure and mechanical properties of the final cellulose material. Results of different characterisation techniques showed that when the cellulose gel was washed with distilled water, it had a significantly higher number of lithium cations (ICP-MS and Raman), amorphous structure (X-ray) and lower mechanical properties (nanoindentation) compared to samples washed with a combination of 2-propanol and deionized water. An increase in viscosity as previously reported and changes in the NMR and IR spectra of DMAc upon LiCl suggested the formation of an ion-dipol complex, where lithium cations reside adjacent to the oxygen of the carbonyl group of DMAc. The formed macrocation $[DMAc_n + Li]^+$ was preserved between cellulose chains in cellulose specimens washed with distilled water and had an essential role in the disruption of initial bonds, thus enhancing mouldability. Electron microscopy (FE-SEM) studies showed that the surface of cellulose after mechanochemical treatment was rough with no presence of fibres.

Keywords Cellulose · Compression moulding · Pressure · *N,N*-dimethylacetamide · Swelling · Mechanical properties

J. Obradovic · H. Wondraczek · P. Fardim (✉)
Laboratory of Fibre and Cellulose Technology, Åbo Akademi, Porthansgatan 3, Turku 20500, Finland
e-mail: pfardim@abo.fi

L. Lassila
Department of Prosthetic Dentistry and Biomaterials Science, University of Turku, Lemminkäisenkatu 2, 20520 Turku, Finland

P. Navard
Mines ParisTech, CEMEF – Centre de Mise en Forme des Matériaux, CNRS UMR 7635, BP 207, 1 rue Claude Daunesse, 06904 Sophia Antipolis Cedex, France

Abbreviations

DMAc	*N,N*-dimethylacetamide
FE-SEM	Field emission scanning electron microscope
ICP-MS	Inductively coupled plasma mass spectroscopy
RSD	Relative standard deviation
SD	Standard deviation

SWDP   Softwood dissolving pulp
WAXD   Wide angle X-ray diffraction

Introduction

Cellulose is an abundant natural polymer suitable for making a large variety of materials and chemicals. Several cellulosic derivatives can be compounded, pelletised and processed, depending on the cellulose derivative and compounding conditions. Some of the classical tools for thermoplastic processing are extrusion, injection or blow moulding, spinning and filming forming (Quintana et al. 2012).

However, the use of these techniques for processing pure cellulose is impossible since the polymorphs of cellulose I and II do not melt. Recently, several attempts were made to shape pure cellulose, mainly wood pulp, without any chemical treatment. One such study is the compression moulding of wood fibre materials. Researchers used only water as a processing aid, and in the end they obtained all-cellulose composite plaques from pulp of high cellulose purity (Nilsson et al. 2010). In another study, cellulose was plasticised, without chemical modification, by the use of the combination of mechanical shear, uniaxial pressure and laser radiation (Schroeter and Felix 2005).

Since cellulose does not melt, processing of cellulose materials is usually based on dissolution in solvents and regeneration to two-dimensional objects such as fibres and films. However, cellulose, among other features, has a complex system of hydrogen bonds that prohibits dissolution of cellulose in common organic and inorganic media. Disruption of the hydrogen bond network can be done mechanically or chemically. Cellulose with a completely amorphous structure is usually prepared by ball milling (Zhang et al. 2007). Another alternative to disrupt the hydrogen bonding network is to use high-pressure treatment. When polymers are subjected to high pressure, a rearrangement at all levels of their structural organisation occurs (Ioelovich 2008). Structural rearrangements in polymers subjected to high pressure may be related to possible changes in the intensity of intermolecular interactions. In the case of cellulose, X-ray diffraction analysis suggests that the crystalline phase may be destroyed, leaving an amorphous state (Zhorin et al. 2010). Beside the mechanical methods, there are several chemical treatments for producing amorphous cellulose. Reported methods are deacetylation of cellulose acetate under non-aqueous alkaline conditions (Wadehra and Manley 1965) and regeneration of cellulose dissolved in different solvent systems (Ciolacu et al. 2011; Volkert and Wagenknecht 2008). The disadvantage with conventional amorphous cellulose is its tendency to recrystallise into cellulose II in the presence of water.

Physical and chemical properties of cellulose are strongly influenced by the arrangement of the cellulose molecules. There are two types of hydrogen bonds present in cellulose fibres, viz., intramolecular interactions occurring between the C-3 OH group and oxygen of the pyranose ring as well as intermolecular hydrogen bonds occurring between the C-6 OH group and oxygen of the glucosidic bond of another molecule. Hydrogen bonds form cellulose crystallites that are very difficult to penetrate by solvent molecules. Furthermore, if the starting material is amorphous cellulose, reactivity of chains will be much higher, for example, the enzymatic hydrolysis of cellulose to glucose (Haan et al. 2007). Besides its high reactivity, amorphous cellulose is necessary for the drawing and shaping process. Togawa and Kondo (1999) investigated the drawing process of cellulose films. In order to achieve a high draw ratio, hydrogen bonds needed to be dissociated during the drawing process. The drawability is hindered by intermolecular hydrogen bonds, since these bonds restrict the mobility of polymer chains. For successful drawing of cellulose films, hydrogen bonds were suppressed prior to the drawing process with a DMAc/LiCl solvent system. Processing of natural materials such as wood or cellulose is not as convenient as processing synthetic polymers. Conventional processing of synthetic polymers involves thermal processing. Higher temperatures in thermal process of natural materials lead to the decomposition of materials before melting. Zhang et al. (2012) presented a process for producing plastic cellulose material without chemical modification or addition of additives. Cellulose powder was ball milled before it was subjected to the back pressure equal channel angular pressure. The purpose of this mechanical pretreatment was to disrupt the cellulose particles and enhance the chain entanglement. The storage modulus was higher for the ball-milled

samples compared to the un-milled ones. The XRD results showed the decrease in crystallinity and crystal size. Crystallinity of cellulose powder was reduced, which allowed production of cellulose plastics under the strong shear-deformation conditions.

The swelling process of cellulose fibres prior to dissolution is an important step in cellulose chemistry and technology. The main part of the interactions of cellulose with an external agent is the change in morphology. The swelling of cellulose in various solvent systems has been the subject of numerous investigations. The heterogeneous swelling of the fibres in chemical mixtures such as sodium hydroxide or N-methylmorpholine N-oxide (NMMO) in water was observed long ago. The same mechanisms were also observed when using solvents such as ionic liquids (Cuissinat et al. 2008) and other chemicals (Cuissinat 2006). From all these studies, it was shown that the key parameter in the dissolution mechanism is the morphology of the fibre. If the original wall structure of the native fibre is preserved, the dissolution mechanisms are mostly similar to those of wood, cotton, and others.

The present research work aims to take advantage of the modifications in the intermolecular interactions, wherein a swelling treatment enables cellulose moulding. Cellulose pulp was thus swollen with a DMAc/LiCl solvent system, washed and dried before further processing. Formability of these treated cellulose samples was evaluated. The objective of this study was to explore the possibilities of moulding pre-swollen cellulose materials and to understand the role of disrupting the intermolecular bonds of cellulose without derivatisation.

Materials and methods

Materials

Softwood dissolving pulp was acquired from Domsjö Fabriker, Sweden. Dissolving pulp is produced from a controlled mixture of spruce and pine (60 %:40 %) by a two-stage sodium-based cooking to give a sulphite pulp with very low lignin content (0.6 %) and high alpha-cellulose content (93 %). The viscosity of pulp was 530 ± 30 ml/g according to the ISO 5351 standard and the degree of polymerisation was 780 (Domsjö 2011). Cellulose was swollen with *N,N*-dimethylacetamide (Sigma-Aldrich, Finland) and lithium chloride (Merck, Finland). Acetone was purchased from J. T. Barker. All chemicals were used as received without further purification.

### Swelling of pulp in the DMAc/LiCl solvent system

The pulp was first chopped into small pieces of 2.0 g each. Swelling of softwood dissolving pulp in DMAc/LiCl involves the following solvent exchange procedure. Initially, each cellulose sample was suspended in 300 cm^3 distilled water for 1 h at room temperature. After filtration, it was immersed into 200 cm^3 acetone for 1 h and subsequently into 100 cm^3 *N,N*-dimethyl-acetamide for 1 h at room temperature; 50 cm^3 DMAc was heated to 40 °C followed by the addition of 3.0 g lithium chloride to the solution. When the swelling procedure was finished, a transparent gel was formed. The gel was solidified by distilled water and exchanged for fresh distilled water after 1, 4 and 12 h. After solidification, the cellulose, referred to hereafter as Cell_DL, was dried at room temperature for further processing. A second solidification procedure involved the washing of a transparent gel with a solvent composed of isopropyl alcohol and deionized water (40:60). Samples were washed twice with 100 ml of this solvent. After washing, the samples were soaked in 300 ml deionized water to remove the residual isopropyl alcohol. Further, to remove the lithium from cellulose, samples were exposed to running tap water overnight (Nayak et al. 2008); the resultant product will be referred to hereafter as Cell_RS. The whole experimental part is depicted in Fig. 1.

Moulding of swollen cellulose specimens

A cylindrical mould (Fig. 2) with a piston was built of stainless steel. A dried sample was put in the mould, closed with the piston and placed on a regular hydraulic press (Enerpac bench press). The sample was pressed at about 70 MPa vertical pressure for a couple of seconds at room temperature (Fig. 3).

Optical microscopy

The swelling mechanism of cellulose in the DMAc/LiCl solvent system was studied with a Nikon Eclipse E200 optic microscope attached to a Nikon DS-Fi2
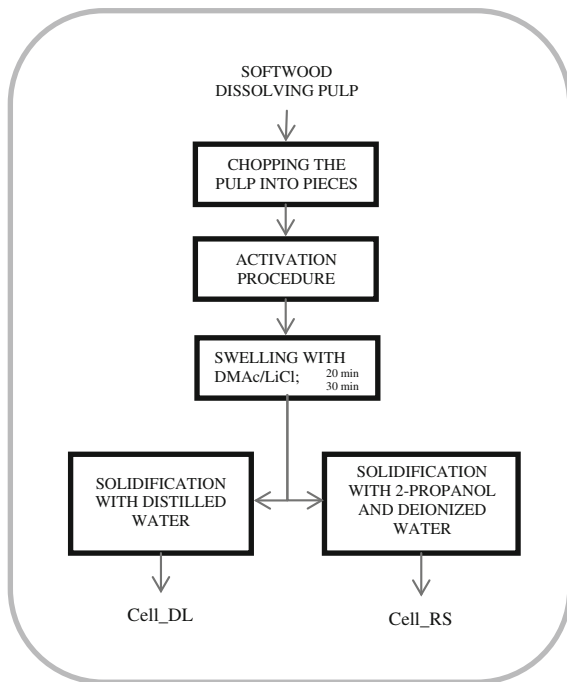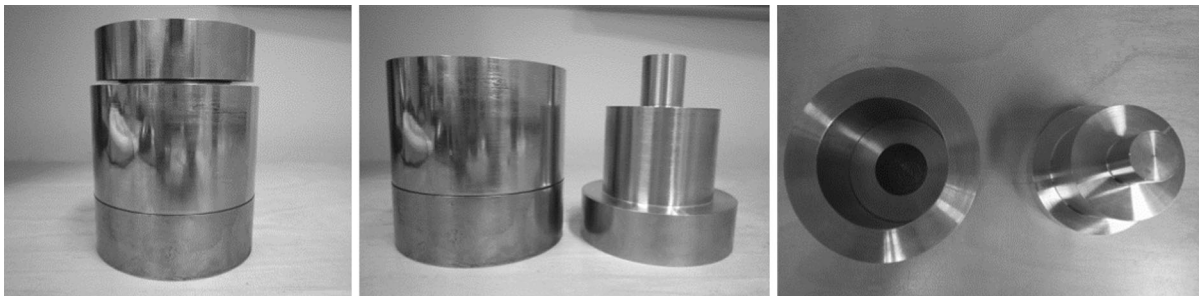
Fig. 1 Schematic representation of the experimental work

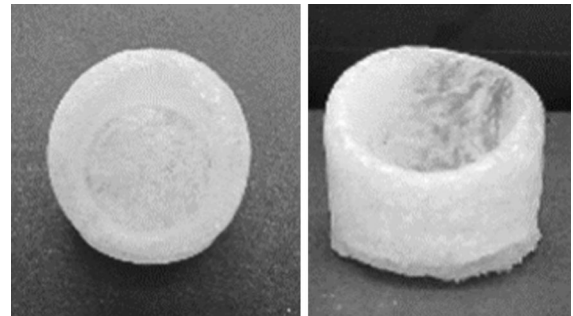Fig. 3 Images of the moulded sample (Cell_DL)

digital camera. Swelling treatment was recorded after 10, 20 and 30 min.

Determination of crystallinity using X-ray diffraction (XRD)

X-ray diffraction measurements were performed on a goniometer (PW3020) using CuKα radiation generated at 30 mA and 40 kV. The CuKα radiation consists of Kα1 (1.54060 nm) and Kα2 (1.54443 nm) components. Dried cellulose samples were cut and put on a plastic substrate. Scans were obtained from 15 to 70°, 2θ degrees in 0.02-degree steps for 1.5 s per step.

Degree of crystallinity (I_c) was calculated from the ratio of the height of the 002 peak (I_{max}) and the height of the minimum between the 002 and 101 peaks, shown in Eq. (1):

$$I_c = 1 - \frac{I_{min}}{I_{max}} \qquad (1)$$

Determination of the cellulose structure using Raman spectroscopy (FT-Raman)

Cellulose samples were analysed with the Thermo Scientific Nicolet iS50 spectrometer. The Raman system is equipped with a 1,064-nm diode laser. The laser power used for chemically treated sample excitation was 500 mW, and 1,024 scans were accumulated. Reference pulp was excited with 0.35 W power, and 32 scans were collected. The Omnic software programme was used to find peak positions and process the spectral data.

Determination of the lithium ion concentration analysed by ICP-MS

The samples were first digested with a microwave digestion system from Anton Paar, Multiwave 3,000.

Fig. 2 Pictures of the prototype stainless steel

Sample amounts were balanced in a range of 0.1 g, and 5 cm^3 65 % HNO$_3$ suprapur from Merck and 1 cm^3 30 % H$_2$O$_2$ suprapur were added. The temperature in the microwave oven was up to 200 °C. The analysis was performed with a ICP-MS from Perkin-Elmer Sciex Elan 6100 DRC+. The standardisation was done with a multistandard from Ultra Scientific, item: IMS-102. The analysing method was the standard performance with the following parameters: sweeps: 11; replicates: 7; dwell time: 100; 10 ppb Rh was used as an internal standard solution.

Field emission scanning electron microscope (FE-SEM)

The morphology of samples was examined by a Leo Gemini 1530 field emission scanning electron microscope with an In-Lens detector. After moulding, samples were dried in air and sectioned using a doctor blade prior to being coated with carbon in a Temcarb TB500 sputter coater (Emscope Laboratories, Ashford, UK). Optimum accelerating voltage was 2.70 kV and magnifications were ×1,500, 10,000, 25,000 and 50,000.

Mechanical characterisation

Mechanical properties of cellulose samples were measured with the UBI1 Nanomechanical Test Instrument (Hysitron, Inc.) using a continuous stiffness measurement in a force-controlled mode with a Berkovich type triangular diamond pyramid. The continuous stiffness measurement technique offers measurements of contact stiffness, hardness, elastic modulus, and creep resistance. The nanoindentation elastic modulus (E) and hardness (H) are defined with the following Eqs. (2) and (3):

$$E = \frac{dP}{dh}\frac{1}{2}\sqrt{\frac{\pi}{A}} \qquad (2)$$

$$H = \frac{P_{max}}{A} \qquad (3)$$

where P_{max} is the applied load at the maximum depth of penetration, A is the contact area, and $\frac{dP}{dh}$ is the slope of the initial portion of the unload curve in the load-displacement plot. Prior to Nanoindentation tests, cellulose samples were pressed with the Pellet Press of FTIR. At least six indentations were made on each sample, with a peak load force of 5,000 μN for the sample where the solvent was removed with 2-propanol and deionized water and 200 μN for the swollen sample washed only with distilled water.

Results

Swelling of cellulose in the DMAc/LiCl solvent system

Swelling of cellulose fibres in the DMAc/LiCl solvent system is also a heterogeneous process. When fibres are placed in DMAc/LiCl, solvent molecules penetrate only to the semipermeable and elastic parts of the fibre wall. The diffused molecules cause radial expansion of the secondary wall. These localised swollen parts along the fibre give the impression of balloons (Navard and Cuissinat 2006). The balloons were formed in the first couple of minutes. In the course of swelling, the balloons were bursting and fragments arise. After 30 min of treatment, a two-phase system was visible. Figure 4 shows that some intact fibres still existed. In the swelling process, Cl$^-$ ions formed hydrogen-type interactions with the hydroxyl group hydrogens of cellulose, breaking the existing bonds in the interior of the structure. Meanwhile, Li$^+$ ions interacted with the carbonyl group oxygen of the DMAc molecule, forming [DMAc$_n$ + Li]$^+$ macrocations. Macrocations acted as a spacer between cellulose chains prohibiting the formation of intermolecular hydrogen bonds. When fibres swell, intermolecular bonds are broken as a result of the stress produced by the swelling process. With a very strong solvent, it is possible to disrupt the entire crystalline structure (Mantanis et al. 1995). In this particular case, 30 min swelling was sufficient to reduce the crystallinity of fibres to the necessary amount to make the moulding process possible. A shorter swelling time would not decrease the crystallinity sufficiently, and this results in a brittle non-mouldable material. A longer swelling time would go to the dissolution stage, where cellulose II would arise.

Effect of swelling treatment on crystallinity analysed by XRD

Native and most regenerated cellulose consists of crystalline and non-crystalline domains. The physical
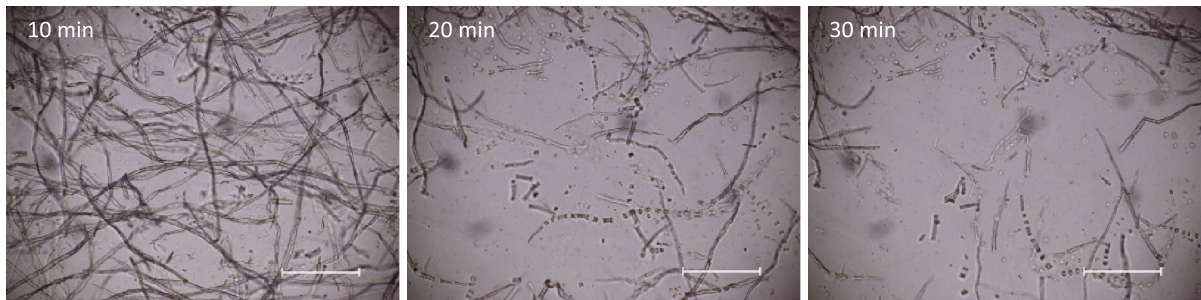
Fig. 4 Optical micrographs during the swelling process of cellulose in the DMAc/LiCl solvent sytem. *Bar* represents 500 μm

Fig. 5 X-ray diffractogram of the reference pulp, swollen cellulose washed with distilled water (Cell_DL) and swollen cellulose washed with a mixture of 2-propanol and deionized water (Cell_RS)
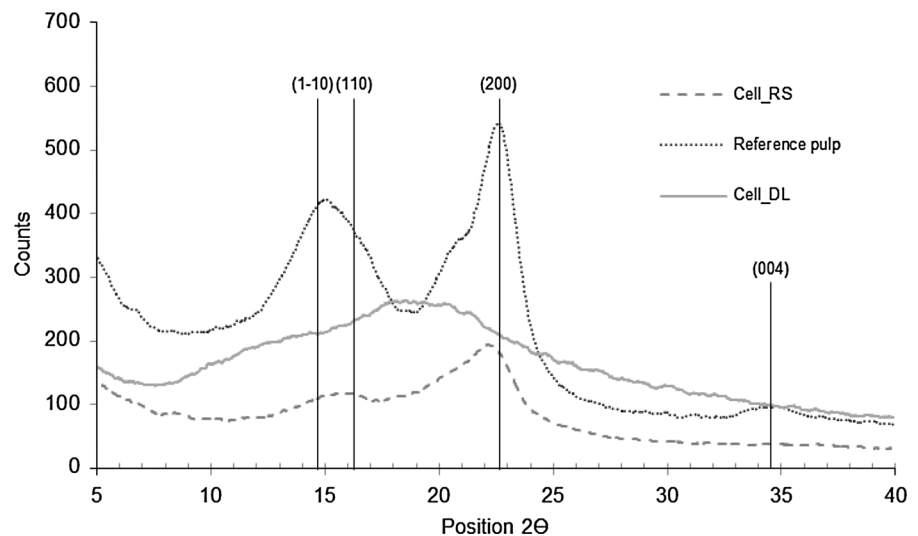

properties and reactivity of cellulose are strongly influenced by the arrangement of cellulose molecules. Interactions between cellulose and reactive substances occur first in non-crystalline domains. The X-ray patterns of the reference pulp, the sample washed with distilled water (Cell_DL) and the sample washed with the organic solvent (Cell_RS) are presented in Fig. 5. The X-ray diffractogram for the reference softwood dissolving pulp had two peaks, characteristic of the cellulose I crystal structure. The crystalline structure of softwood pulp was lost after swelling in DMAc/LiCl and solidifying with distilled water. Duchemin et al. (2007) studied the transformation of microcrystalline cellulose due to partial dissolution in 8 % DMAc/LiCl. His work helped to understand the phase transformation that occurs during dissolution in this particular solvent system. Dissolution occurs through the continuous peeling of layers of crystal domains. The peeled layers may retain some of the cellulose I structure from which they were removed, but

generally they are too thin to contain crystallite chains. This is why the precipitated peeled layers seemed to be amorphous cellulose. Significant crystalline diffraction was not observed in Cell_DL specimens, indicating that the slow solidification of samples in distilled water produced crystallites of small size or with imperfections in the crystalline structure. The Cell_RS specimen has diffraction peaks at 15.0° and 22.3°, indicating a cellulose I structure. Although the sample had the same crystallinity pattern as native cellulose, the swelling treatment resulted in a decrease in the degree of crystallinity from 0.54 to 0.43.

Effect of the swelling treatment on the cellulose structure analysed by FT-Raman

Raman spectra in the frequency region of 300–3,700 cm^{-1} for the reference pulp, Cell_DL and Cell_RS are shown in Fig. 6, which indicates the spectral changes occurred upon the loss of

Fig. 6 Raman spectra for the reference pulp, swollen cellulose washed with distilled water (Cell_DL) and swollen cellulose washed with a mixture of 2-propanol and deionized water (Cell_RS)
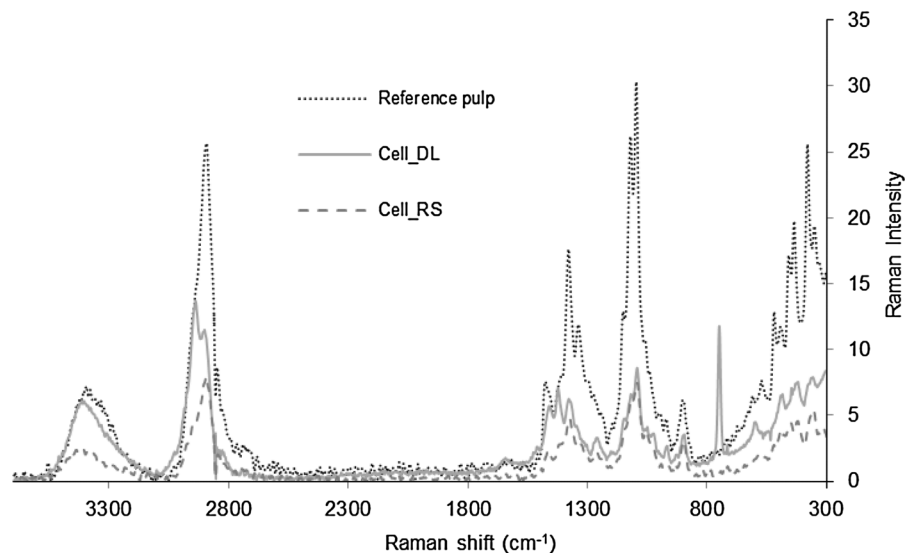
crystallinity. Between 1,000 and 1,200 cm^{-1}, there are ring bond stretches and C–O stretches. The angle bends (CCC, OCC, COC, OCO), C–O stretches and methylene bending appear between 700 and 800 cm^{-1}. Between 400 and 600 cm^{-1} are the heavy atom bending, C–O and ring bending, and some ring stretching. Between 200 and 400 cm^{-1} are ring torsions. The spectrum of a crystalline substance contains sharp discrete bands, whereas the amorphous materials contain broad diffuse bands (Socrates 2001). The broad band in the 3,100–3,600 cm^{-1} region that was due to the OH-stretching vibrations gave information concerning the hydrogen bonds. The peak characteristic of hydrogen bonds from the Cell_DL sample became wider in comparison to the peak from the reference pulp, which can be correlated with the interruption of the intra- and intermolecular hydrogen bond by swelling treatment. The Cell_DL spectrum exhibits a strong band at 605 cm^{-1}, which is due to the bending motion of the O=C–N group of the DMAc molecule. The amide I band characteristic for the C=O stretching vibration can be seen at 1,650 cm^{-1}. This band is a typical carbonyl adsorption band of tertiary amides. The Raman spectrum from the Cell_RS sample was similar to the reference pulp, except for the missing 605 and 1,650 cm^{-1} peaks. In general, all amides have one or more bands of medium-to-strong intensity, which may be broad, in the 695–550 cm^{-1} region, which are probably due to the bending motion of the O=C–N group. The carbonyl absorption band of tertiary amides occurs in the 1,670–1,630 cm^{-1}

region. The lack of these two peaks indicates the absence of DMAc in Cell_RS samples.

Lithium residual analysed by ICP-MS

The concentration of Li ions in cellulose samples was measured with inductively coupled plasma mass spectroscopy as a function of treatment time in the solvent. As shown in the Table 1, the Li$^+$ ion concentration revealed that after swelling with DMAc/LiCl, cellulose samples contained more lithium ions than the reference soft dissolving pulp. The small size of Li$^+$ ions allows them to interact with glucan chains, including more restricted regions near the oxygen linkers. The concentration of Li$^+$ ions decreased from 672.04 to 526.98 ppm with a decrease of the swelling time from 30 to 20 min. It can be concluded that Li$^+$ ions stayed between the cellulose chains, and the amount of Li$^+$ ions is affected by the swelling time. Specimens solidified with 2-propanol and deionized water had significantly lower amounts of lithium ions, indicating that the solvent removed most of the cations. Taking into account the results from Raman spectroscopy of the Cell_RS specimen, it can be concluded that most of the DMAc/LiCl is expelled. This is in agreement with the findings of Nayak et al. (2008). Their study showed an insignificant amount of DMAc and Li$^+$ ions (10.61 ppm) present in the films even after washing with a 2-propanol and deionized water mixture, subjecting it to running water. The observed difference between

Table 1 Determination of the lithium ion concentration with ICP-MS for the reference pulp, cellulose containing DMAc/LiCl (Cell_DL) and cellulose from which DMAc/LiCl had been removed (Cell_RS)

Sample	Content (mg/kg)	SD (mg/kg)	RSD (%)
Reference	0.02	0.01	64.90
Cell_DL, 30 min	672.04	17.80	2.60
Cell_DL, 20 min	526.98	8.73	1.20
Cell_RS, 30 min	1.79	0.02	1.30

the Cell_DL and Cell_RS samples regarding the content of retained lithium cations might be due to the final exposure to water. The time the Cell_DL samples spent in a beaker with distilled water was 29 h in total, while Cell_RS samples were exposed to running water over night. Even before the exposure to water, the Cell_RS sample had a lower amount of macrocation. Most of the macrocation had already been washed with an anti-solvent composed of 2-propanol and deionized water. This solvent has a lot more power in dissociating cellulose with the solvent complex.

Effects of swelling treatment on the morphology of fibres analysed by FE-SEM

The morphological structure of cellulose samples treated with DMAc/LiCl and moulded was observed using scanning electron microscopy. The scanning electron micrographs (Fig. 7) showed the heterogeneous and rough surface of moulded cellulose samples. This is consistent with the findings of Yun et al. (2008). In their study, curing of cellulose previously dissolved in DMAc/LiCl with deionized water led to objects with a wrinkled rough surface and non-homogeneously generated layered structure. FE-SEM images (Fig. 8) demonstrate the microfibril bundle structure. A similar discovery was reported by Wei and Cheng (2007) when they studied the effect of solvent exchange on the structure of cellulose. They concluded that solvent activation prior to dissolution of cellulose led to the fibrillation of the treated fibre surface. These findings indicated that the chemical and mechanical treatment of cellulose caused destruction of the cell wall organisation and led to re-organisation of microfibrils into layers. Fibrils are destroyed by swelling treatment and reassembled in a whole new structure. SEM images of Cell_RS samples were not
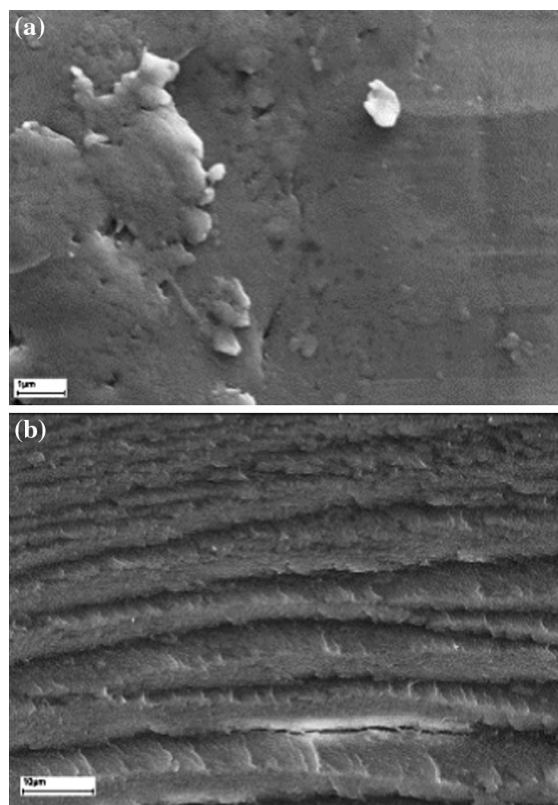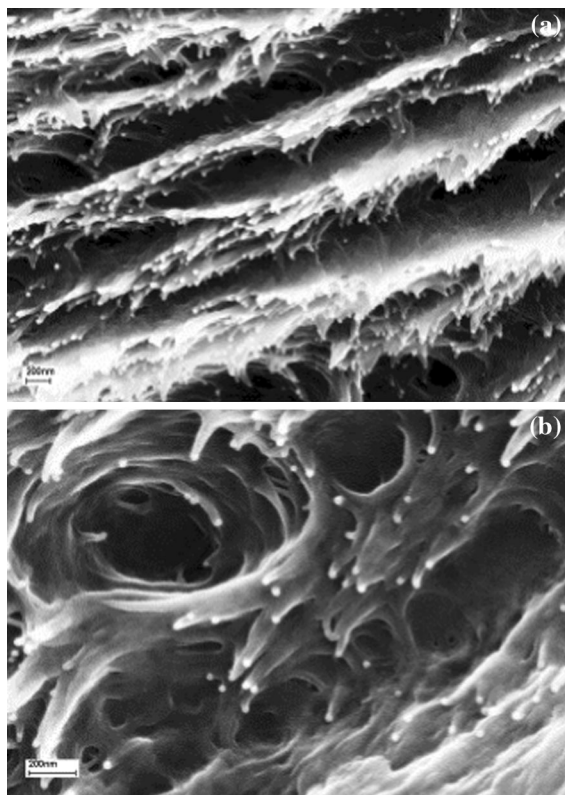
Fig. 7 SEM images of the swollen cellulose surface of Cell_DL [magnification (**a**) ×10,000 and (**b**) ×1,500]

taken because it was not possible to perform the moulding step.

Mechanical properties

The nanoindentation tests were used to investigate the mechanical properties of the cellulose sample. The elastic modulus and hardness of specimens measured by nanoindentation are shown in Table 2. The surface roughness had an impact on the measurement especially for the shallow penetrations, so the average values were calculated from the 18th to 33rd cycle. Both the hardness and elastic modulus were significantly higher in Cell_RS than in Cell_DL. The results of the mechanical testing for Cell_DL samples were expected since the speciments had an amorphous structure, which made them less rigid, weaker and easily deformed. The solvent trapped in samples affects the surface morphology and mechanical properties of the material. Trapped $[DMAc_n + Li]^+$ macrocations hinder cellulose from forming an ordered

Fig. 8 SEM cross-sectional images of the swollen cellulose Cell_DL [magnification (**a**) ×25,000 and (**b**) ×50,000]

Table 2 Mechanical properties measured with nanoindentation for cellulose containing DMAc/LiCl (Cell_DL) and cellulose from which DMAc/LiCl had been removed (Cell_RS)

Sample	Elastic modulus (MPa)	Hardness (MPa)	Force (μN)	Depth (nm)	Cycle
Cell_DL	54	6.5	200	3,932	33
Cell_RS	6,993	381.4	5,000	2,839	33

structure by weakening the intermolecular hydrogen bonds between cellulose chains, which results in low mechanical properties (Yun et al. 2008). Cellulose samples with crystalline structures have higher hardness and elastic moduli. Increased crystallinity is associated with an increase in rigidity and hardness. Our results suggest that disruption of the hydrogen bonding network via intermolecular noncovalent bonding allows the preparation of mouldable cellulose.

Conclusions

The objective of this study was to prepare mouldable cellulose materials without chemical modification. Cellulose swelling is essential for producing cellulose products. The DMAc/LiCl solvent system was used to swell cellulose with the aim to broaden its application in producing functional materials. The swelling process was necessary to break the existing bonds in the interior of the structure, thus lowering the crystallinity of cellulose fibres. Reduced crystallinity can be diminished even more by preserving the solvent between cellulose chains. This can be accomplished using distilled water as an anti-solvent. Retained swelling solvent acted as a spacer between cellulose chains prohibiting formation of intermolecular hydrogen bonds. Separated cellulose chains had a disordered structure, which made them ductile and easily deformed. If the solvent was washed away from specimens with a mixture of isopropyl alcohol and deionized water, intermolecular hydrogen bonds were reformed. In this case, the material became brittle and lost its ability to be moulded. Three-dimensional cellulose objects can be produced only if the DMAc/LiCl solvent system is present in the cellulose specimens. Our future research will focus on alternatives to mimic this behaviour using solvents/agents that are easier to recycle and upscale to industrial applications.

References

Ciolacu D, Ciolacu F, Popa IV (2011) Amorphous cellulose-structure and characterization. Cellulose Chem Technol 45:13–21

Cuissinat C (2006) Swelling and dissolution mechanisms of native cellulose fibres. PhD dissertation, Ecole Nationale Supérieure des Mines de Paris, Sophia-Antipolis, France

Cuissinat C, Navard P, Heinze T (2008) Swelling and dissolution of cellulose, Part IV: free floating cotton and wood fibres in ionic liquids. Carbohydr Polym 72:590–596

Domsjö (2011) Specification Domsjö cellulose. http://www.domsjoe.com. Accessed 01 Feb 2012

Duchemin BZ, Newman HR, Staiger PM (2007) Phase transformation in microcrystalline cellulose due to partial dissolution. Cellulose 14:311–320. doi:10.1007/s10570-007-9121-4

Haan DR, Rose SH, Lynd LR, van Zyl WH (2007) Hydrolysis and fermentation of amorphous cellulose by recombinant Saccharomyces cerevisiae. Metab Eng 9(1):87–94

Ioelovich M (2008) Cellulose as a nanostructured polymer: a short review. Bioresources 3:1403–1418

Mantanis GI, Young RA, Rowell RM (1995) Swelling of compressed cellulose fiber webs in organic liquids. Cellulose 2:1–22

Navard P, Cuissinat C (2006). Cellulose swelling and dissolution as a tool to study the fiber structure. 7th International symposium alternative cellulose: manufacturing, forming, properties. Rudolstadt, Germany

Nayak NJ, Chen Y, Kim J (2008) Removal of impurities from cellulose films after their regeneration from cellulose dissolved in DMAc/LiCl solvent system. Eng Chem Res 47:1702–1706

Nilsson H, Galland S, Larsson TP, Gamstedt KE, Nishino T, Berglund AL, Iversen T (2010) A non-solvent approach for high-stiffness all-cellulose biocomposites based on pure wood cellulose. Compos Sci Technol 70:1704–1712. doi:10.1016/j.compscitech.2010.06.016

Quintana R, Persenaire O, Bonnaud L, Dubois P (2012) Recent advances in (reactive) melt processing of cellulose acetate and related biodegradable bio-compositions. Polym Chem 3:591–595. doi:10.1039/C1PY00421B

Schroeter J, Felix F (2005) Melting cellulose. Cellulose 12:159–165. doi:10.1007/s10570-004-0344-3

Socrates G (2001) Infrared and Raman characteristic group frequencies, 3rd edn. Wiley, West Sussex

Togawa E, Kondo T (1999) Change of morphological properties in drawing water-swollen cellulose films from organic solutions. A view of molecular orientation in the drawing process. J Polym Sci 37:451–459

Volkert B, Wagenknecht W (2008) Substitution patterns of cellulose ethers- Influence of the synthetic pathway. Macromol Symp 262:97–118

Wadehra IL, Manley J (1965) Recrystallization of amorphous cellulose. J Appl Polym Sci 9:2627–2630

Wei Y, Cheng F (2007) Effect of solvent exchange on the structure and rheological properties of cellulose in LiCl/DMAc. J Appl Polym Sci 106:3624–3630. doi:10.1002/app.26886

Yun S, Chen Y, Nayak NJ, Kim J (2008) Effect of solvent mixture on properties and performance of electro-active paper made with regenerated cellulose. Sens Actuators B: Chem 29:652–658. doi:10.1016/j.snb.2007.09.049

Zhang W, Liang M, Lu C (2007) Morphological and structural development of hardwood cellulose during mechano-chemical pretreatment in solid state through pan-milling. Cellulose 14:447–456. doi:10.1007/s10570-9135-y

Zhang X, Wu X, Gao D, Xia K (2012) Bulk cellulose plastic materials from processing cellulose powder using bulk pressure-equal channel angular pressing. Carbohydr Polym 87:2470–2476

Zhorin AV, Kiselev RM, Zelenetskii NA, Rudakova AT (2010) Calorimetric investigation of some polysaccharides subjected to high-pressure plastic deformation. Polym Sci 52:398–406. doi:10.1134/s0565545x10040085